

EXTRACTION OF DAMAGED BUILDINGS USING HIGH-RESOLUTION SATELLITE IMAGES IN THE 2006 CENTRAL JAVA EARTHQUAKE

Kazuki Matsumoto¹, Tuong Thuy Vu², and Fumio Yamazaki³

¹Graduate Student, ²Post-Doctoral Research Fellow, ³Professor
Department of Urban Environment Systems, Chiba University
1-33 Yayoi-cho, Inage-ku, Chiba, 263-8522, Japan
+81-43-290-3528, +81-43-290-3558

kazukim@graduate.chiba-u.jp, thuyvu@as.tu.chiba-u.ac.jp, yamazaki@tu.chiba-u.ac.jp

KEY WORDS: 2006 Central Java Earthquake, Damage Detection, Object-based Classification, High-resolution Satellite.

ABSTRACT: The Central Java Earthquake with magnitude 6.3 occurred on May 27, 2006. Due to this earthquake, about 5,800 people were killed and about 38,000 people were injured. In this study, using QuickBird images, acquired before and after the earthquake, we attempted to extract the areas of building damage based on object-based classification. In land cover classification using high-resolution satellite images by pixel-based classification, salt-and-paper noise occurs. This problem may be solved by object-based classification. First, building areas were extracted for the pre-event image and the post-event image by pixel-based classification. Secondly, the similar extractions were conducted by object-based classification and the results from the two methods were compared. Finally, taking the difference of the building areas for the pre- and post-event images by the object-based approach, damaged building areas were identified and the result was compared with that by visual inspection.

1. INTRODUCTION

It is very important to grasp an extent of damage in an early stage, after the occurrence of natural disasters. Because of advance of remote sensing technology, we can recently get high-resolution satellite image, e.g. QuickBird and Ikonos, in which we can identify a house or a car, as well as moderate resolution satellite images, shortly after a disaster occurs. In the 2004 Indian Ocean Tsunami, a large number of remotely sensed images acquired before and after the tsunami were used very effectively in rescue and restoration activities. In this way, remotely sensed images became one of the important sources to grasp damage distribution in broad areas.

Using a post-event Ikonos image and pre-event other satellite images, Saito et al. (2004) performed visual damage inspection of Bhuj area after the 26 January 2001 Gujarat, India earthquake. They compared the satellite images and the photos taken in a field survey and discussed the accuracy of high-resolution satellite images in building damage detection. Yamazaki et al. (2004) conducted visual interpretation of individual building damage using QuickBird images, taken both before and after the 2003 Boumerdes, Algeria, Earthquake. Based on European Macroseismic Scale (EMS-98), they discussed the variation of damage interpretation results depending on interpreters. Yano et al. (2004) also carried out similar visual damage inspection for the 2003 Bam, Iran, Earthquake.

Although visual damage inspection provides very useful information, it is time consuming.

Therefore image processing methods have been employed to quickly perform damage interpretation. The most standard approach along this line is pixel-based land cover classification based on, e.g., the maximum likelihood method. However, for high-resolution images, pixel-based approaches may give too noisy results because of their too-high resolution. Mitomi et al. (2002) developed a method to detect debris using edge information from post-disaster aerial images. After a pixel-based debris extraction, they performed a texture analysis to reduce “salt and pepper noise”.

To solve the salt-and pepper problem in high-resolution images, object-based classification has recently been introduced. Kouchi et al. (2005) compared the result from pixel-based classification and that from object-based one for debris detection using QuickBird images in the 2003 Boumerdes, Algeria, Earthquake. In this study, however, only the post-event image was used and thus, pre-event information, e.g. location of buildings, was not used effectively.

In this paper, usefulness of object-based classification is further investigated in building damage detection from high-resolution satellite images obtained before and after the 2006 Central Java Earthquake. Building areas are extracted for both pre-event and post-event images by pixel-based and object-based classifications. The results from the two methods are compared and by taking the difference of the building areas from the pre- and post-event images, the areas of damaged buildings are identified and the results are compared with that by visual inspection.

2. THE 2006 CENTRAL JAVA EARTHQUAKE AND QUICKBIRD IMAGES

A strong earthquake of magnitude 6.3 struck Java Island, Indonesia on May 27, 2006 at 5:54 am local time. The epicenter was located at 7.962°S, 110.458°E, about 25 km south-southeast of Yogyakarta with the depth was 10km (Fig.1). Due to this earthquake, about 5,800 people were killed and about 38,000 people were injured. About 140,000 houses were collapsed and about 190,000 houses were heavily damaged (USGS, UNOSAT).

QuickBird image has very high resolution, 0.6m per pixel (panchromatic-mode) and 2.4m per pixel (multi-spectral-mode) and has 4 bands: blue, green, red, near-infrared. After the Java Earthquake, QuickBird capture a clear image of affected areas on June 13, 2006. The image includes Imogiri, one of the most severely affected areas in this earthquake. For the area, a pre-event image on July 11, 2003 also exists. Thus the present authors purchased these images and they were used in this study.

First, pan-sharpened images of 0.6m resolution were produced through combining panchromatic images and multi-spectral images as shown in Fig. 2. Next, the registration was carried out between these pre- and post-event images using RST transformation method and Nearest Neighbor resampling. This process is quite important since the subtraction is carried out between the outcomes from these two images.

3. DETECTION OF BUILDING AREAS

3.1 Pixel-based Classification

First, conventional pixel-based classification was carried out based on the maximum likelihood

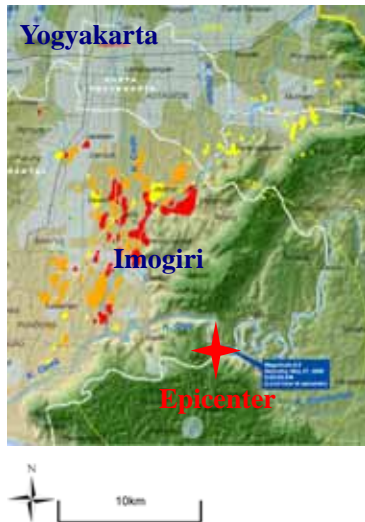
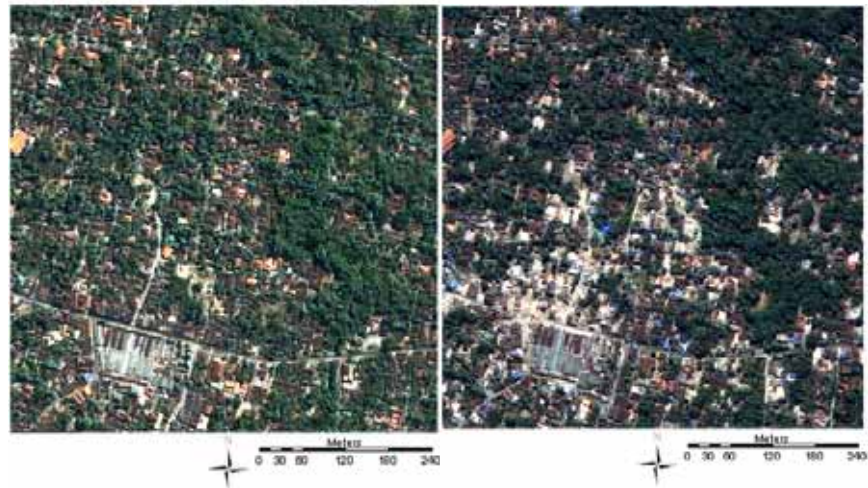


Figure 1. Epicenter in the 2006 Central Java Earthquake (UNOSAT)



(a) July 11, 2003

(b) June 13, 2006

Figure 2. Pan-sharpened natural color images of Imogiri

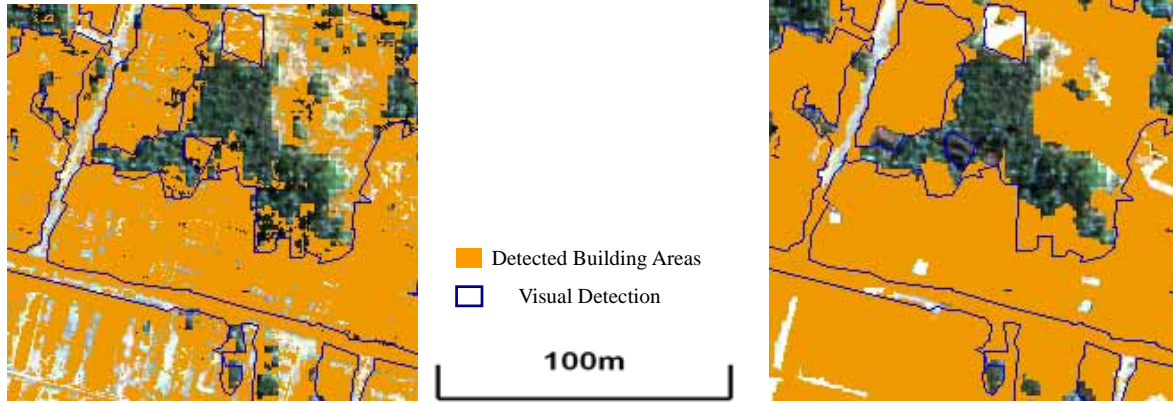
method, the most common supervised classification method. In the classification, 8-bit data value of blue, green, red, and near-infrared bands were used. The following 8 classes: black-roof, gray-roof, red-roof, white-roof buildings, road, soil, vegetation, and shadow, were assigned for the pre-event image as training data. For the post-event image, 7 classes: black-roof, gray-roof, red-roof buildings, debris, road, vegetation, and shadow, were assigned. White-roof building and soil classes were not used for the post-event image since they look difficult to select training data and also they look close to debris class. The building areas obtained by the pixel-based classification are shown in Fig. 3 (a) and Fig. 4 (a). In these figures, the buildings with different roof-color are shown in the same color for easier understanding.

3.2 Object-based Classification

In performing object-based classification, e-Cognition software was used. First, image segmentation was conducted to make “objects” using the pre-event and post-event images. In e-Cognition, the segmentation process is determined by 5 parameters: *Layer Weight*, *Compact Weight*, *Smooth Weight*, *Shape Factor*, and *Scale Parameter* (Baatz et al., 2004). The most important parameter is *Scale Parameter*, which determines the object size. The *Shape Factor* is to determine the important level of spectral heterogeneity or shape heterogeneity in segmentation. When the shape factor moves toward 0, spectral heterogeneity is more concerned. On the contrary, if it moves toward 0.9, shape heterogeneity is more concerned. In further details, the spectral heterogeneity is decided by *Layer Weight*, which gives the weight for each band. And the shape heterogeneity is decided by *Compact Weight* and *Smooth Weight*. The bigger the *Compact Weight* is, the segmented objects are in more compact shape. Alternatively, the bigger the *Smooth Weight* is, the segmented objects are in more smooth shape. Starting from pixels, segmentation runs the merge between two objects and is terminated when a condition is reached. This condition is defined based on the fusion value f , which measures the changes when merging and decided by *Layer Weight*, *Compact Weight*, *Smooth Weight*, *Shape Factor*. If f equals or becomes bigger than the squared *Scale Parameter*, the condition is reached. Although it is difficult to decide the appropriate parameters suitable to all land cover classes, the user can decide the suitable parameters to a few focused classes, e.g. building, road.

Table 1. Parameters used for image segmentation

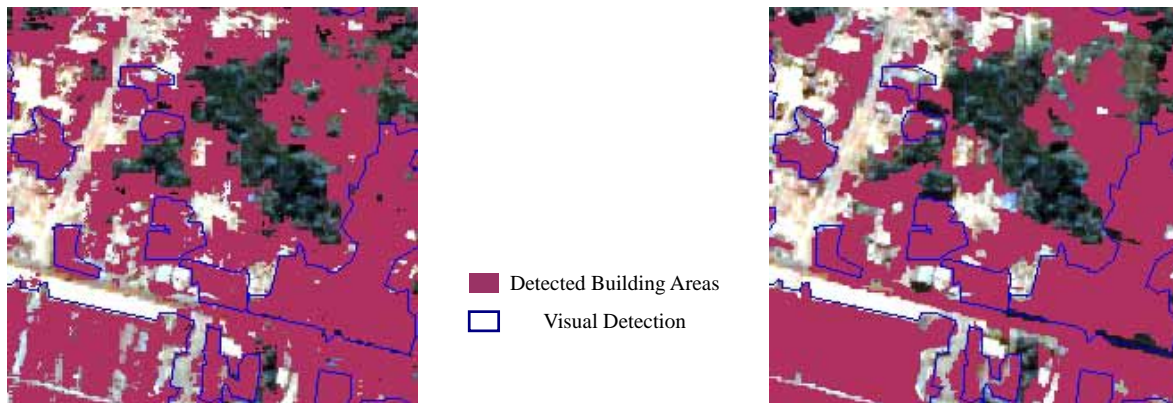
	<i>Layer Weight</i>	<i>Compact Weight</i>	<i>Smooth Weight</i>	<i>Shape Factor</i>	<i>Scale Parameter</i>
Pre-event Image	1	0	1	0.9	8
Post-event Image	1	0.1	0.9	0.8	5



(a) Pixel-based

(b) Object-based

Figure 3. A part of building areas detected for the pre-event image



(a) Pixel-based

(b) object-based

Figure 4. A part of building areas detected for the post-event image (the same area as Fig. 3)

The appropriate parameters for buildings shown in Table 1 were used and image segmentation was conducted for the pre-event and post-event images. Then, the samples for all the classes were selected as the same areas in the pixel-based classification. The objects' mean values of blue, green, red, and near-infrared were used as the indices of classification and the nearest neighbor classification method was selected. The results from the object-based classification for the pre-event and post-event images are shown in Fig. 3 (b) and Fig. 4 (b), respectively. Comparing the results from the pixel-based and object-based classifications with that by visual inspection, salt-and-paper noises are seen in the pixel-based classification. Hence, it may be concluded that in this resolution and the sizes of the target objects, the better result can be acquired by object-based classification. But in object-based classification, some road and shadow areas were misclassified to the building classes because their spectral values of the sample area are similar to those of the building classes. Hence even object-based classification, some classes like these are needed to remove in advance using object feature indices, e.g. length, or spatial relationships.

4. DETECTION OF DAMAGED BUILDING AREAS

In this study, the areas with damaged buildings were identified using the pre-event and post-event building areas, extracted by object-based classification. The subtraction of the post-event building area from the pre-event building area, the rest is considered to be changed (collapsed) building areas. Some other possibilities can also be considered; vegetation or shadow covered over the buildings in the post-event image, and the buildings have removed after acquiring the pre-event image. The first case was considered by removing the vegetation or shadow covered post-event areas (Fig. 5) from the pre-event building areas. The second case was not adjusted assuming that building removals in this 3-year period were mostly due to damages from the earthquake.

The identified building damage areas are shown in Fig. 6 for a small area, and in Fig. 7 for the whole study area. Comparing the result by the image processing described above and that by visual inspection, a reasonable level of accuracy is seen in Fig. 6. However, some omission errors and commission errors are also observed. Accuracy of the proposed method was evaluated using the concept of producer accuracy and user accuracy, defined in Fig. 8. Producer accuracy was obtained as 67.4%, and user accuracy as 51.5% for the whole study area shown in Fig. 7.

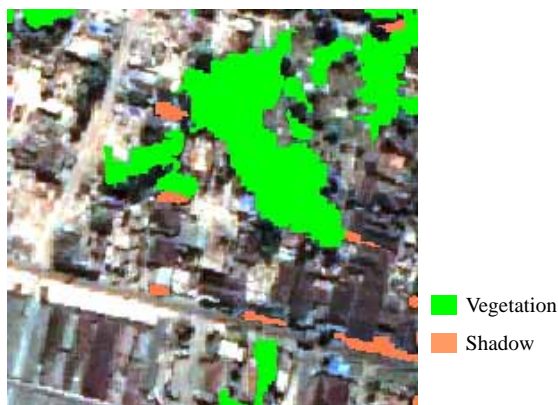


Figure 5. A part of detected vegetation and shadow areas (the same area as Fig. 3)

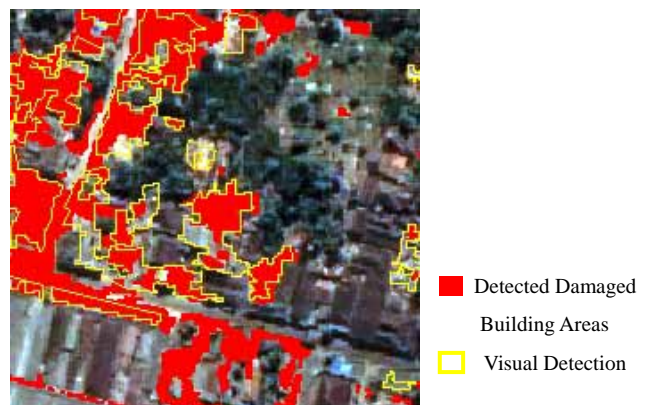


Figure 6. A part of detected damaged building areas (the same area as Fig. 3)



(a) Automated (b) Visual
Figure 7. Damaged building areas

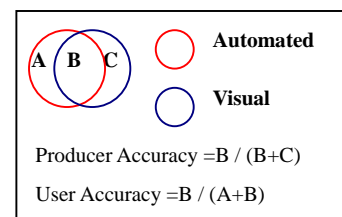


Figure 8. Concept of producer accuracy and user accuracy

5. CONCLUSION

Automated detection of the areas with building damage was conducted using QuickBird images captured before and after the 27th May 2006 Central Java Earthquake. First, building areas were detected by pixel-based classification and object-based classification methods for both pre-event and post-event images. Because salt-and pepper noises were seen in the pixel-based classification result, the object-based classification is considered to be more suitable to identify the areas covered by buildings in high-resolution satellite images. But the result by the object-based classification includes some misclassifications, and thus some additional process may be necessary. Finally, taking the difference of the building areas for the pre- and post-event images by the object-based approach, damaged building areas were identified and the result was compared with that by visual inspection. A reasonable level of accuracy was observed by this comparison. To establish a general damage detection method in future, however, more parametric studies must be necessary for various urban and rural environments.

ACKNOWLEDGMENTS

This study was partially supported by the Ministry of Education, Science, Sports and Culture (MEXT), Japan through Grant-in-Aid for Special Purposes, No.1890001, 2006. QuickBird images used in this study are owned by DigitalGlobe, Inc.

REFERENCES

- Baatz, M., Benz, U., et al., 2004. Definiens Imaging, e-Cognition user guide 4, pp. 76-78.
- European Seismological Commission, 1998. European Macroseismic Scale 1998.
- Kouchi, K., and Yamazaki, F., 2005. Damage Detection Based on Object-based Segmentation and Classification from High-resolution Satellite Images for the 2003 Boumerdes, Algeria Earthquake, Proceedings of 26th Asian Conference on Remote Sensing, CD-ROM, pp. 6.
- Mitomi, H., Matsuoka, M., and Yamazaki, F., 2002. Application of Automated Damage Detection of Buildings due to Earthquakes by Panchromatic Television Images, The 7th U.S National Conferences on Earthquake Engineering, CD-ROM, pp. 10.
- Saito, K., Spence, R.J.S., Going, C., and Markus, M., 2004. Using high-resolution satellite images for post-earthquake building damage assessment: a study following the 26 January 2001 Gujarat Earthquake, Earthquake Spectra, Vol. 20, No. 1, pp. 145–169.
- UNOSAT, URL: <http://unosat.web.cern.ch/unosat/>
- USGS, URL: <http://earthquake.usgs.gov/eqcenter/eqinthenews/2006/usneb6/>
- Yamazaki, F., Kouchi, K., Kohiyama, M., Matsuoka, M., and Muraoka, N., 2004. Damage Detection from High-resolution Satellite Images for the 2003 Boumerdes, Algeria Earthquake, Proceedings of the 13th World Conference on Earthquake Engineering, CD-ROM, Paper No.2595, pp. 13.
- Yano, Y., Yamazaki, F., Matsuoka, M., and Vu, T., T., 2004. Building Damage Detection of the 2003 Bam, Iran Earthquake using QuickBird Images, Proceedings of 25th Asian Conferences on Remote Sensing, pp. 618-623.